Inorganic Chemistry
Article

Inorg. Chem. **2009**, *48*, 6409–6416 **6409**
DOI: 10.1021/ic900069r

Excited-State Dynamics in a Dyad Comprising Terpyridine-Platinum(II) Ethynylene Linked to Pyrrolidino-[60]Fullerene

Barbara Ventura,*,† Andrea Barbieri,† Alberto Zanelli,† Francesco Barigelletti,† Julie Batcha Seneclauze,‡ Stéphane Diring,‡ and Raymond Ziessel*,‡

†*Istituto per la Sintesi Organica e la Fotoreattività, Consiglio Nazionale delle Ricerche (ISOF-CNR), Via P. Gobetti 101, 40129 Bologna, Italy, and* ‡*Laboratoire de Chimie Organique et Spectroscopies Avancées, Ecole de Chimie, Polymères, Matériaux (ECPM), Université de Strasbourg, 25 rue Becquerel, 67087 Strasbourg Cedex 02, France*

Received January 14, 2009

A hybrid [Pt(^{t}Bu$_3$terpy)(C≡C—Ph—C$_{60}$)]$^+$ complex (**Pt**−**Fu**) wherein a phosphorescent platinum center is linked to fullerene has been prepared using a copper(I)-promoted cross-coupling reaction. The electrochemical and spectroscopic properties were understood in light of the properties of the isolated building blocks and references compounds, **Pt** and **Fu**. In particular, in **Pt**−**Fu**, the electrochemical studies revealed that the first reduction process is fullerene-based and that the lowest-energy Pt$^+$−Fu$^-$ charge-separated (CS) state lies in the range 2.0−2.1 eV. The luminescence properties of the investigated species have been monitored in a CH_2Cl_2 solvent at room temperature and in a MeOH/EtOH (1:4 v/v) glassy solution at 77 K. Upon excitation at 450 nm at room temperature and in air-free solvent, **Pt** displays an intense luminescence of ^{3}MLCT nature, with λ_{max} = 605 nm (523 nm at 77 K, corresponding to 2.37 eV), ϕ_{em} = 0.013, and τ_{em} = 920 ns. Under the same conditions, **Fu** exhibits the typical $^1C_{60}$ fluorescence, with λ_{max} = 708 nm (703 nm at 77 K, corresponding to 1.76 eV), $\phi_{em} = 6.0 \times 10^{-4}$, and τ_{em} = 1.2 ns. For **Pt**−**Fu**, room-temperature excitation at 450 nm yields Pt*- and Fu*-centered excited states in a 1.2:1 proportion. However, no Pt-based emission is observed, and (i) in an air-free solvent, ^{1}Fu fluorescence is observed, while (ii) in an air-equilibrated solvent, singlet oxygen sensitization by the ^{3}Fu level takes place. Very close $^1O_2$* fluorescence intensities are observed at 1278 nm for isoabsorbing solutions at 450 nm of **Fu** and **Pt**−**Fu**, consistent with complete Pt → Fu energy transfer in the dyad. The room-temperature nanosecond transient absorption spectra for **Pt**−**Fu** and **Fu** exhibit peaks at 680 and 690 nm with τ_{TA} = 14.3 and 24.8 μs, respectively; in both cases, these are attributed to absorption by the fullerene triplet. By contrast, no CS species, Pt$^+$−Fu$^-$, are detected. The Pt → Fu energy transfer is discussed, and the rate constant for the ^{3}Pt−Fu → Pt−^{1}Fu step is evaluated, $k_{en} > 10^7$ s^{-1}.

Introduction

Pt(II) complexes based on functionalized terpyridine (terpy) ligands constitute an expanding class of compounds with interesting photophysical properties; terpy is 2,2′:6′,2″-terpyridine.[1−3] In particular, it is remarkable that the Pt → terpy charge-transfer (^{3}MLCT) luminescence, that is, its energy, intensity, and lifetime, can be tuned to a large extent, depending on the functional groups appended at the terpy frame. This property renders the complexes amenable to several applications, ranging from sensing[4] to energy conversion functionalities.[5−8] Pt(II) terpyridyl acetylides exhibit additional interesting spectroscopic properties, a consequence of the strong-field effect brought about by an acetylide ligand in the fourth coordination position.[9−14]

*To whom correspondence should be addressed. E-mail: bventura@isof.cnr.it (B.V.), ziessel@chimie.u-strasbg.fr (R.Z.).

(1) Williams, J. A. G. *Top. Curr. Chem.* **2007**, *281*, 205–268.
(2) McMillin, D. R.; Moore, J. J. *Coord. Chem. Rev.* **2002**, *229*, 113–121.
(3) Eryazici, I.; Moorefield, C. N.; Newkome, G. R. *Chem. Rev.* **2008**, *108*, 1834–1895.
(4) Wong, K. M. C.; Tang, W. S.; Chu, B. W. K.; Zhu, N. Y.; Yam, V. W. W. *Organometallics* **2004**, *23*, 3459–3465.
(5) Chan, S. C.; Chan, M. C. W.; Wang, Y.; Che, C. M.; Cheung, K. K.; Zhu, N. Y. *Chem.—Eur. J.* **2001**, *7*, 4180–4190.
(6) Geary, E. A. M.; Yellowlees, L. J.; Jack, L. A.; Oswald, I. D. H.; Parsons, S.; Hirata, N.; Durrant, J. R.; Robertson, N. *Inorg. Chem.* **2005**, *44*, 242–250.
(7) Islam, A.; Sugihara, H.; Hara, K.; Singh, L. P.; Katoh, R.; Yanagida, M.; Takahashi, Y.; Murata, S.; Arakawa, H. *Inorg. Chem.* **2001**, *40*, 5371–5380.
(8) Chakraborty, S.; Wadas, T. J.; Hester, H.; Schmehl, R.; Eisenberg, R. *Inorg. Chem.* **2005**, *44*, 6865–6878.
(9) Castellano, F. N.; Pomestchenko, I. E.; Shikhova, E.; Hua, F.; Muro, M. L.; Rajapakse, N. *Coord. Chem. Rev.* **2006**, *250*, 1819–1828.
(10) Rachford, A. A.; Goeb, S.; Ziessel, R.; Castellano, F. N. *Inorg. Chem.* **2008**, *47*, 4348–4355.
(11) Shikhova, E.; Danilov, E. O.; Kinayyigit, S.; Pomestchenko, I. E.; Tregubov, A. D.; Camerel, F.; Retailleau, P.; Ziessel, R.; Castellano, F. N. *Inorg. Chem.* **2007**, *46*, 3038–3048.
(12) Yam, V. W. W.; Tang, R. P. L.; Wong, K. M. C.; Cheung, K. K. *Organometallics* **2001**, *20*, 4476−4482.
(13) Yang, Q. Z.; Wu, L. Z.; Wu, Z. X.; Zhang, L. P.; Tung, C. H. *Inorg. Chem.* **2002**, *41*, 5653–5655.
(14) Ziessel, R.; Diring, S.; Retailleau, P. *Dalton Trans.* **2006**, 3285–3290.

Published on Web 06/15/2009

Because of its electron-donating ability, the acetylide ligand causes a low-energy displacement of the lowest-lying Pt → terpy CT level and a concomitant increase of the metal-centered d−d energy separation, all of this resulting in significant improvements of the luminescence parameters, particularly of the intensity.[1]

Fullerene moieties as part of supramolecular systems have long been subject to extensive studies, among others, in view of applications related to energy conversion.[15−21] Fullerene C_{60} is known to be a very good electron acceptor, as indicated by its first reduction potential (for several of its derivatives, $E_{1/2}^{red}$ is in the range −0.6 to −0.8 V vs saturated calomel reference electrode (SCE)).[22] On this basis, provided thermodynamic requirements related to the electron transfer steps can be fulfilled, systems yielding charge-separated (CS) states upon action of light can be devised. This can be done by coupling fullerene moieties with suitable light absorbing units or assemblies, designed to play as oxidizable counterparts.[15,23−26] Among the several photoactive partners employed, polypyridine complexes of Ru(II), Re(I) and Cu(I),[26,27] and Ir(III)[28] have been recently used to build dyads comprising the C_{60} moiety. These latter studies have been very useful because they have contributed to calling attention to the role of the lowest-lying singlet and triplet levels of localized $^1C_{60}$ and $^3C_{60}$ nature. Actually, in these cases following the fast sequence of steps originated from the light absorbing event, these fullerene-centered levels appear to be effectively populated, which represents a detrimental occurrence against the potential utilization of the energy stored in CS levels.

This paper deals with the first case, wherein a Pt(II)−terpyridine unit might play such a donor role in a fulleropyrrolidine−acetylide−platinum(II)−terpyridyl dyad (**Pt−Fu**), Chart 1. Here, we report on the preparation, characterization, and study of the nature of the processes and excited states originated by light absorption at the dyad **Pt−Fu**. To this aim, we compare its electrochemical, luminescence, and transient absorption properties with those of the reference component units, **Pt** and **Fu**, respectively, whose schematic structures are shown in Chart 1; the properties of the **PtCl** precursor, Chart 1, have been likewise investigated. In particular, we find that, within **Pt−Fu**, Pt → Fu energy transfer is by far the predominant if not exclusive photoinduced event. This happens because population of the charge-separated state Pt^+-Fu^- appears disfavored in terms of the energy layout of the various involved excited levels.

Chart 1. Schematic Structure of Dyad **Pt−Fu** and Model Compounds

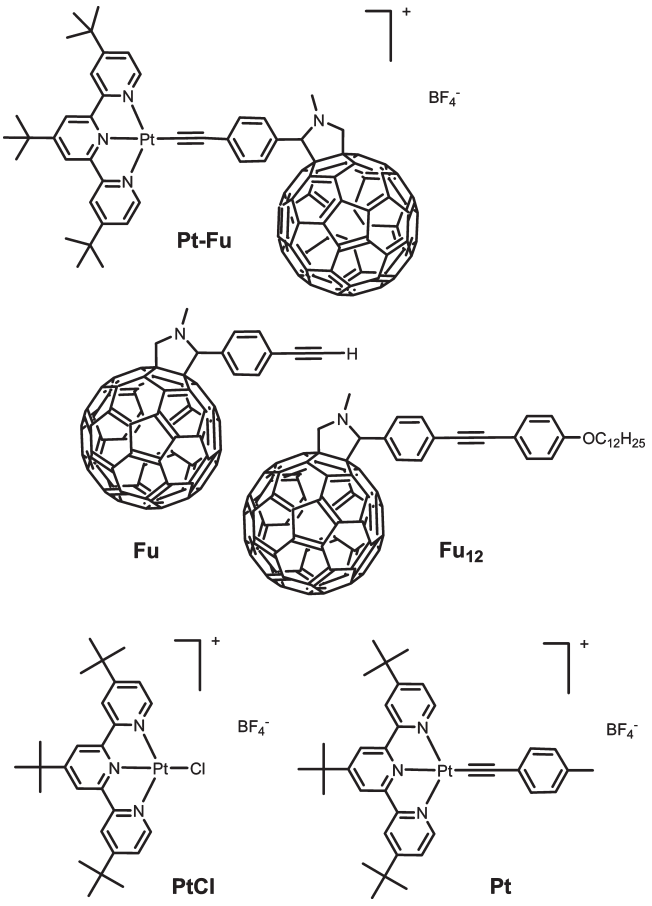

Experimental Section

General Methods. The 400.1 (^{1}H) and 100.3 (^{13}C) MHz NMR spectra were recorded at room temperature using perdeuterated solvents as internal standards: δ (H) in parts per million relative to residual protiated solvent; δ (C) in parts per million relative to the solvent. FT-IR spectra were recorded on the neat liquids or as thin films, prepared with a drop of dichloromethane and evaporated to dryness on KBr pellets. Chromatographic purification was conducted using standardized flash silica gel. Thin-layer chromatography was performed on aluminum oxide or silica plates coated with a fluorescent indicator. All mixtures of solvents are given as volume/volume (v/v) ratios.

Electrochemical Measurements. Electrochemical studies employed cyclic voltammetry with a conventional three-electrode system using a BAS CV-50W voltammetric analyzer equipped with a Pt microdisk (2 mm^2) working electrode and a silver wire counter-electrode. Ferrocene was used as an internal standard and was calibrated against a SCE separated from the electrolysis cell by a glass frit presoaked with an electrolyte solution. Solutions contained the electro-active substrate in deoxygenated and anhydrous dichloromethane/*o*-dichlorobenzene containing tetra-*n*-butylammonium hexafluorophosphate (0.1 M) as a supporting electrolyte. The quoted half-wave potentials were reproducible within ~10 mV.

(15) Imahori, H.; Sakata, Y. *Eur. J. Org. Chem.* **1999**, 2445–2457.
(16) Prato, M. *J. Mater. Chem.* **1997**, *7*, 1097–1109.
(17) Foote, C. S. *Top. Curr. Chem.* **1994**, *169*, 347–363.
(18) Vail, S. A.; Schuster, D. I.; Guldi, D. M.; Isosomppi, M.; Tkachenko, N.; Lemmetyinen, H.; Palkar, A.; Echegoyen, L.; Chen, X. H.; Zhang, J. Z. H. *J. Phys. Chem. B* **2006**, *110*, 14155–14166.
(19) Segura, J. L.; Martin, N.; Guldi, D. M. *Chem. Soc. Rev.* **2005**, *34*, 31–47.
(20) Martin, N.; Sanchez, L.; Herranz, M. A.; Guldi, D. M. *J. Phys. Chem. A* **2000**, *104*, 4648–4657.
(21) Schuster, D. I.; Cheng, P.; Jarowski, P. D.; Guldi, D. M.; Luo, C. P.; Echegoyen, L.; Pyo, S.; Holzwarth, A. R.; Braslavsky, S. E.; Williams, R. M.; Klihm, G. *J. Am. Chem. Soc.* **2004**, *126*, 7257–7270.
(22) Echegoyen, L.; Echegoyen, L. E. *Acc. Chem. Res.* **1998**, *31*, 593–601.
(23) Guo, F. Q.; Ogawa, K.; Kim, Y. G.; Danilov, E. O.; Castellano, F. N.; Reynolds, J. R.; Schanze, K. S. *Phys. Chem. Chem. Phys.* **2007**, *9*, 2724–2734.
(24) Yamanaka, K. I.; Fujitsuka, M.; Araki, Y.; Ito, O.; Aoshima, T.; Fukushima, T.; Miyashi, T. *J. Phys. Chem. A* **2004**, *108*, 250–256.
(25) Matsumoto, K.; Fujitsuka, M.; Sato, T.; Onodera, S.; Ito, O. *J. Phys. Chem. B* **2000**, *104*, 11632–11638.
(26) Armaroli, N.; Accorsi, G.; Clifford, J. N.; Eckert, J. F.; Nierengarten, J. F. *Chem. Asian J.* **2006**, *1*, 564–574.
(27) Armaroli, N.; Accorsi, G.; Felder, D.; Nierengarten, J. F. *Chem.—Eur. J.* **2002**, *8*, 2314–2323.
(28) Nastasi, F.; Puntoriero, F.; Campagna, S.; Schergna, S.; Maggini, M.; Cardinali, F.; Delavaux-Nicot, W.; Nierengarten, J. F. *Chem. Commun.* **2007**, 3556–3558.

Materials. The platinum complexes [(^{t}Bu$_3$terpy)PtCl]BF$_4$,[29] [(^{t}Bu$_3$−terpy)PtC≡CTol]BF$_4$,[11] 4-ethynylbenzaldehyde,[30] and the fullerene derivative *N*-methyl-2-(4′-ethynyl)phenyl-3,4-fulleropyrrolidine[31] were synthesized according to literature procedures.

Synthesis. 4-(2-(4-(Dodecyloxy)phenyl)ethynyl)benzaldehyde (HOC—Ph-≡-Ph—OC$_{12}$H$_{25}$). A mixture of 4-ethynylbenzaldehyde (125 mg, 0.36 mmol), 1-(dodecyloxy)-4-iodobenzene (52 mg, 0.4 mmol), and Pd(PPh$_3$)$_2$Cl$_2$ (15 mg, 0.02 mmol) in THF (10 mL) and triethylamine (3 mL) was degassed vigorously by bubbling argon through the solution; then, the CuI (7 mg, 0.04 mmol) was added. The solution was stirred at room temperature for one weekend. The solvent was removed by rotary evaporation. The residue was treated with water and extracted with dichloromethane. The organic extracts were washed with water and dried over absorbent cotton. The solvent was removed by rotary evaporation. The residue was purified by chromatography on silica gel with petrol ether/ethylacetate (75:15) as an eluant. Ultimate washing with pentane offers 4-(2-(4-(dodecyloxy)phenyl)ethynyl)benzaldehyde (100 mg, 70%). ^{1}H NMR (200 MHz, CDCl$_3$): δ 10.00 (s, 1H), 7.87 (d, 2H; J = 7.7 Hz), 7.64 (d, 2H; J = 8.0 Hz), 7.48 (d, 2H; J = 8.0 Hz), 6.89 (d, 2H; J = 8.0 Hz), 4.0 (t, 2H; J = 6.0 Hz), 1.79 (m, 2H), 1.26 (m, 18H), 0.88 (m, 3H).

***N*-Methyl-2-(4′-(2-(4-(dodecyloxy)phenyl)ethynyl)phenyl-3,4-fulleropyrrolidine (Fu$_{12}$).** A mixture of 4-(2-(4-(dodecyloxy)-phenyl)ethynyl)benzaldehyde (78 mg, 0.2 mmol), C$_{60}$ (190 mg, 0.2 mmol), and *N*-methylglycine (36 mg, 0.4 mmol) was refluxed for 24 h in toluene. After cooling to room temperature, the solvent was evaporated under vacuum conditions, and the residue was purified on a silica gel column, eluting with a gradient of petroleum ether (30−0%) in toluene, recovering as the first band the unreacted [60]fullerene (120 mg), followed by the reaction product (40 mg, yield 46%). ^{1}H NMR (200 MHz, CDCl$_3$): δ 7.80 (m, 2H), 7.58 (d, 2H; J = 8.4 Hz), 7.43 (d, 2H; J = 8.4 Hz), 6.84 (d, 2H; J = 8.8 Hz), 5.0 (d, 1H; J = 9.1 Hz), 4.99 (s, 1H), 4.30 (d, 1H; J = 9.1 Hz), 3.95 (t, 2H; J = 6.4 Hz), 2.85 (s, 3H), 1.77 (m, 2H), 1.26 (m, 16H), 0.84 (m, 5H). ^{13}C NMR (100 MHz, CDCl$_3$): δ 165.5, 165.2, 164.6, 163.0, 160.2, 159.5, 159.2, 147.5, 146.5, 146.1, 145.7, 145.7, 145.5, 145.5, 145.4, 144.6, 142.8, 142.4, 142.2, 142.1, 141.9, 136.7, 133.2, 132.0, 129.5, 114.7, 109.5, 104.7, 101.4, 98.2, 93.3, 87.9, 77.6, 77.2, 76.7, 69.2, 68.3, 53.6, 40.2, 37.3, 32.1, 29.8, 29.7, 29.5, 29.3, 26.2, 22.8, 14.3. FT-IR (ATR): ν = 3739 (w), 2921 (s), 2849 (s), 2783 (m), 2120 (m, $\nu_{C\equiv C}$), 2084 (m, $\nu_{C\equiv C}$), 1735 (m), 1601 (m), 1514 (m), 1461(m), 1428 (w), 1332 (w), 1432 (m), 1246 (s), 1173 (m), 1103 (s), 1019 (s), 828 (m), 801 (s). EI-MS: m/z 1137.1 (100%, [M]). Anal. calcd for C$_{89}$H$_{39}$NO (M_r = 1138.27): C, 93.91; H, 3.45; N, 1.23. Found: C, 94.24; H, 2.84; N, 1.18.

[(^{t}Bu$_3$−terpy)Pt(C$_{60}$-ϕ-≡)]BF$_4$ (Pt−Fu). The preparation began with the dissolution of [(^{t}Bu$_3$−terpy)PtCl](Cl) (26 mg, 0.54 mmol) in toluene (5 mL) and a mixture of DMF (4 mL) and triethylamine (3 mL), followed by the addition of *N*-methyl-2-(4′-ethynyl)phenyl-3,4-fulleropyrrolidine (**Fu**; 52 mg, 0.059 mmol). The solution was degassed vigorously by bubbling argon through the solution. Then, the CuI (0.8 mg, 0.04 mmol) was added. After stirring at room temperature for three days, the solvent was removed by rotary evaporation. Purification was ensured by column chromatography using alumina as a solid support and a gradient of methanol (0−2%) in dichloromethane as a mobile phase; the solvent was evaporated under vacuum conditions, and the residue was dissolved in a minimum of DMSO (2 mL) and filtrated over Celite and dropped into an aqueous solution (10 mL) containing NaBF$_4$ (1.200 g). The complex was recovered by filtration over paper, washed with water (3 × 100 mL), and the red solid dried under high vacuum conditions. Ultimate recrystallization by the slow evaporation of dichloromethane and pentane from a dichloromethane/toluene/pentane solution afforded complex **Pt−Fu** (0.202 g, 88%). ^{1}H NMR (400 MHz, CDCl$_3$): δ 9.15 (d, 2H; J = 6.2 Hz), 8.45 (s, 2H), 8.38 (s, 2H), 7.79 (m, 2H), 7.61 (d, 2H; J = 6.2 Hz), 7.57 (d, 2H; J = 8.7 Hz), 5.0 (d, 1H; J = 9.5 Hz), 4.96 (s, 1H), 4.29 (d, 1H; J = 9.1 Hz), 2.84 (s, 3H), 1.59 (s, 9H), 1.49 (s, 18H). ^{13}C NMR (100 MHz, CDCl$_3$): δ 168.9, 167.7, 159.0, 154.2, 154.4, 147.5, 147.0, 146.4, 146.3, 146.1, 146.0, 145.7, 145.5, 145.4, 145.0, 144.7, 144.6, 144.5, 143.3, 143.2, 142.8, 142.4, 142.4, 142.3, 142.3, 142.2, 142.1, 141.9, 141.7, 140.3, 140.0, 139.7, 136.1, 125.5, 123.3, 121.8, 104.5, 83.6, 70.2, 69.3, 53.6 (CH$_2$Cl$_2$), 40.2, 37.6, 36.6, 30.6, 30.3. FT-IR (ATR): ν = 3396 (w), 2956 (s), 2921 (s), 2851 (s), 2111 (w, $\nu_{C\equiv C}$), 1728 (m), 1611 (m), 1463 (m), 1373 (w), 1260 (m), 1068 (m), 1018 (m), 798 (m). FAB$^+$: m/z (nature of the peak, relative intensity) 1473.2 ([M]$^+$, 100), 1472.2 ([M]$^+$, 85), 1471.2 ([M]$^+$, 40). Anal. calcd for C$_{98}$H$_{45}$N$_4$PtBF$_4$ + CH$_2$Cl$_2$ (M_r = 1560.32 + 84.93): C, 72.27; H, 2.88; N, 3.41. Found: C, 71.89; H, 2.59; N, 3.25.

Optical Spectroscopy. UV−vis absorption spectra of CH$_2$Cl$_2$ dilute solutions (2×10^{-5} M) of the compounds were obtained with a Perkin-Elmer Lambda 950 spectrometer. The luminescence spectra for CH$_2$Cl$_2$ solutions at room temperature (absorbance < 0.15 at the excitation wavelength) and at 77 K in MeOH/EtOH (1:4 v/v) glassy solutions were measured by using a Spex Fluorolog II spectrofluorimeter with excitation wavelengths λ_{exc} = 330 and 450 nm. Luminescence quantum efficiencies (ϕ_{em}) were evaluated by comparing wavelength-integrated corrected intensities (I) with reference to [Ru(bpy)$_3$]Cl$_2$ (ϕ_r = 0.028, air-equilibrated water)[32] and quinine sulfate (ϕ_r = 0.546, 1 N H$_2$SO$_4$, air-equilibrated)[33] by using the following equation:[34]

$$\phi_{em} = \frac{I(1-10^{-A_r})n^2}{I_r(1-10^{-A})n_r^2}\phi_r \qquad (1)$$

where A and n are the absorbance value at the employed excitation wavelength and the refractive index of the solvent, respectively. The $^1O_2$* luminescence band centered at 1278 nm was monitored by employing an Edinburgh FLS920 spectrometer equipped with a Hamamatsu R5509-72 supercooled photomultiplier tube (193 K), a TM300 emission monochromator with a near-IR grating blazed at 1000 nm, and a Xe900-450-W xenon arc lamp as the light source, λ_{exc} = 450 nm. The luminescence profiles gathered with the luminescence equipment were corrected by using a calibration curve provided by the manufacturer. Excitation spectra were also obtained at the different luminescence peaks; however, their use was not very useful given the extended overlap of the Pt and Fu absorption features. The luminescence lifetimes of the complexes were obtained with an IBH 5000F single-photon apparatus by using nanoled excitation sources at 331 and 465 nm; a nanoled at 560 nm was employed for exclusive excitation of the Fu center in the dyad. Analysis of the luminescence decay profiles against time was accomplished by using software provided by the manufacturer. Estimated errors are 2 nm on band maxima, 20% on quantum yields, and 10% on lifetimes, and the working temperature was either 295 ± 2 K (1 cm square optical cells employed) or 77 K (with samples contained in capillary tubes immersed in liquid nitrogen).

Transient absorption spectra in the nanosecond−microsecond time domain were obtained by using the nanosecond flash photolysis apparatus Proteus manufactured by Ultrafast Systems LLC. The excitation source was the third harmonic (355 nm) of a Continuum Surelite II Nd:YAG laser tuned to 450 nm with a Continuum Surelite OPO system, with 5 ns pulse duration at 1.5 mJ/pulse. Light signals were passed through a Chromex/Bruker 500IS monochromator (equipped with two gratings blazed at 600 or 1200 nm) and collected on a high-speed Silicon (DET210)

(29) Yip, H. K.; Cheng, L. K.; Cheung, K. K.; Che, C. M. *J. Chem. Soc., Dalton Trans.* **1993**, 2933–2938.
(30) Thorand, S.; Krause, N. *J. Org. Chem.* **1998**, *63*, 8551–8553.
(31) Lembo, A.; Tagliatesta, P.; Guldi, D. M. *J. Phys. Chem. A* **2006**, *110*, 11424–11434.
(32) Nakamaru, K. *Bull. Chem. Soc. Jpn.* **1982**, *55*, 2967.
(33) Eaton, D. F. *Pure Appl. Chem.* **1988**, *60*, 1107–1114.
(34) Demas, J. N.; Crosby, G. A. *J. Phys. Chem.* **1971**, *75*, 991.

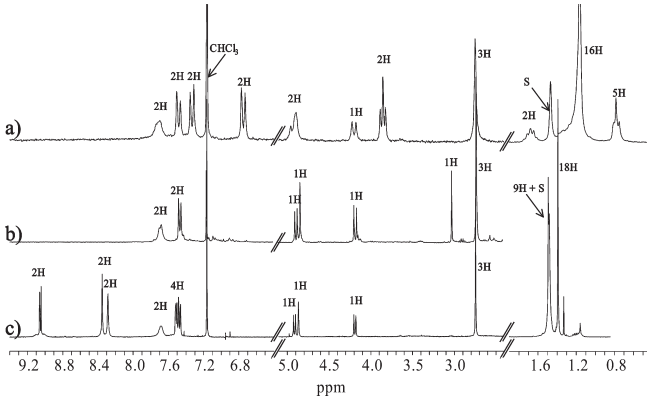

Figure 1. Proton NMR (400.1 MHz) spectra measured in $CDCl_3$ at room temperature for **Fu_{12}** (a), **Fu** (b), and **Pt−Fu** (c). S accounts for residual water.

or InGaAs (DET410) Thorlabs detector in the VIS (400−800 nm) and NIR (800−1700 nm) regions, respectively. The signal was then amplified by means of a variable gain wideband voltage amplifier (Femto DHPVA-200) interfaced with a Tektronix TDS 3032B digital oscilloscope connected to a PC having the acquisition software Proteus. The probe light source was a Spectra Physics 69907 150 W CW Xe Arc lamp. The samples were placed in home-modified 1 cm fluorescence cells and purged from oxygen by bubbling for 10 min with a stream of argon.

Results and Discussion

Synthesis. The target **Pt−Fu** dyad was prepared by cross-coupling the fullerene **Fu** with the **PtCl** precursor in the presence of triethylamine as a base. This reaction is promoted by CuI (10 mol %) in the strict absence of oxygen. During the reaction, the color of the solution turned deep-brown, and a red solid progressively deposited. At the end of the reaction (2 days), anion exchange is ensured using an excess of $NaBF_4$ in water. Recrystallization of the remaining solid afforded the desired complex in 88% yield. This complex was unambiguously characterized by NMR, IR, and MS spectroscopies and elemental analysis. In particular, its proton NMR (Figure 1) was compared with that of the **Fu** precursor. The three most deshielded patterns belong to the complexed terpy ligand with the most shifted doublet at 9.15 ppm, with characteristic ^{195}Pt satellites to the 6,6″ protons in the ortho position to the chelating fragment. The most diagnostic signals are those that relate to the ethynyl-C_{60} protons, with a broad two-proton signal belonging to the phenyl protons close to the Fu subunit. These signals for the ortho-hydrogen atoms of the phenyl group contiguous with the pyrrolidine ring appear broad at room temperature due to the known free (restricted) rotation of the phenyl group in phenylpyrrolidinofullerenes, and coalescence could be observed by variable-temperature NMR study.[35] The pyrrolidone protons (two doublets and one singlet) are little shifted compared to **Fu**. The absence of the C≡CH resonance at 3.09 ppm is in keeping with the coupling of the alkyne to the Pt center. The two signals at 1.59 and 1.49 ppm are typical of the tertio butyl protons. The two ethynyl carbons resonate at 104.5 and 83.6 ppm. Changing the phenyl substitution in **Fu**, **Fu_{12}**, and **Pt−Fu** induces a weak chemical shift, allowing postulation that little extension of the conjugation from the Fu to the Pt(terpy) moieties is occurring. Such an observation is further confirmed by determining the redox properties of each residue in the dyad.

Table 1. Electrochemical Data for the Fullerene Molecules and Pt Complexes[a]

	E_{ap} (ox, soln) (V), ΔE (mV)	$E^{0\prime}$ (red, soln) (V), ΔE (mV)
Pt	+1.44 (irr.)	−0.99 (80), −1.55(80)
Fu_{12}	+1.35 (irr.)	−0.71 (65), −1.10 (70), −1.64 (80)[b]
Pt−Fu	+1.42 (irr.)[c]	−0.77 (60); −1.05 (70), −1.13 (70), −1.57 (80), −1.70 (70), −1.96 (80)

[a] Potentials determined by cyclic voltammetry in a deoxygenated 50:50 CH_2Cl_2/*o*-$C_6H_4Cl_2$ v/v solution, containing 0.1 M $TBAPF_6$ (electrochemical window from +1.6 to −2.2 V), at a solute concentration of ca. 1.0 mM and at room temperature, using a scan rate of 200 mV/s unless otherwise indicated. Potentials were standardized versus ferrocene (Fc) as an internal reference and converted to the SCE scale assuming that $E_{1/2}$ (Fc/Fc^+) = +0.38 V (ΔE_p = 60 mV) vs SCE. For reversible processes, $E_{1/2}$ = ($E_{pa} + E_{pc}$)/2; E_{pa} and E_{pc} are anodic and cathodic peak potentials, respectively. The error in half-wave potentials is ±10 mV. For irreversible processes, the peak potentials (E_{ap}) are quoted. All reversible redox steps result from one-electron processes, except as otherwise quoted. [b] Two-electron process. [c] Two irreversible peaks at ≈+1.42 and ≈+1.36 V were resolved using DMF and 0.01 M $TBAClO_4$ as the supporting electrolyte. The cathodic part is mixed up due to the presence of trace amounts of water.

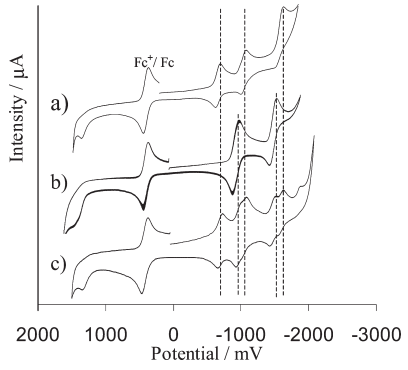

Figure 2. Cyclic voltammetry in 50:50 CH_2Cl_2/*o*-$C_6H_4Cl_2$ v/v containing 0.1 M tetrabutylammonium hexafluorophosphate at room temperature; scan rate, 200 mVs^{-1}. All calibrated against ferrocene (Fc^+/Fc) at $E_{1/2}$ = +0.38 V vs SCE: (a) **Fu_{12}**, (b) **Pt**, (c) **Pt−Fu**.

Electrochemistry. The electrochemical data of the compounds in this study are summarized in Table 1. Due to the insolubility of **Fu** at a millimolar concentration, the soluble **Fu_{12}** has been used as a reference unit. All of the compounds show one irreversible oxidation potential (Figure 2). The oxidation potential of **Pt** at +1.44 V, assigned to a HOMO-centered oxidation, predominantly metal-based, that is, from Pt(II) to Pt(III),[36,37] appears at least 100 mV more positive compared to the fullerene derivatives. No oxidation process could be observed beyond +1.5 V due to the limited potential range of the electrolytic solution.

For **Fu_{12}**, the oxidation at +1.35 V is also observed in similar compounds[31,38] and is probably due to the oxidation of the tertiary amine of the pyrrolidine five-member

(35) Ajamaa, F.; Duarte, T. M. F.; Bourgogne, C.; Holler, M.; Fowler, P. W.; Nierengarten, J. F. *Eur. J. Org. Chem.* **2005**, 3766–3774.

(36) Blanton, C. B.; Murtaza, Z.; Shaver, R. J.; Rillema, D. P. *Inorg. Chem.* **1992**, *31*, 3230–3235.

(37) Von Zelewsky, A.; Gremaud, G. *Helv. Chim. Acta* **1988**, *71*, 1108–1115.

(38) Baffreau, J.; Leroy-Lhez, S.; Van Anh, N.; Williams, R. M.; Hudhomme, P. *Chem.—Eur. J.* **2008**, *14*, 4974–4992.

ring. Notice that, in the dyad **Pt**−**Fu**, the irreversible oxidation lies at the same potential as for **Fu$_{12}$** (Table 1 and Figure 2).

The reference Pt complex displays two reversible couples at ca. −0.99 V and −1.55 V versus SCE arising mainly from the terpyridine reductions with some mixing of Pt(II) metal character.[39,40]

Within the electro-activity window, the **Fu$_{12}$** displays three reversible processes, the third process being dielectronic (Figure 2). The target **Pt**−**Fu** dyad undergoes six reversible reduction process which could be assigned in light of the behavior of the reference compounds **Fu$_{12}$** and **Pt**. Clearly, the first reduction in **Pt**−**Fu** is fullerene-based at −0.77 V, and the second goes to the Pt(terpy) fragment. The second reduction of the fullerene moiety occurs at −1.13 V, whereas the second reduction of the Pt(terpy) fragment occurs at −1.57 V. Then, the additional reduction of the fullerene, appearing in the reference as a dielectronic process is split into two monoelectronic processes at −1.70 and −1.96 V (Figure 2). As shown in Figure 2, the $E_{1/2}$ values for the reduction of the Pt(terpy) and Fu fragments in **Pt**−**Fu** are virtually identical to those of the individual moieties. Such data suggest that the Pt and Fu units behave as weakly interacting modules retaining their own electronic properties, with the exception of the sixth reduced state. From the reported data, in the **Pt**−**Fu** dyad system, the HOMO−LUMO gap (Pt- and Fu-based, respectively) is evaluated to be 2.19 eV.

Spectroscopy. The absorption spectrum of **Pt**−**Fu** and those of the related species investigated are shown in Figure 3. The absorption spectrum of **Pt**−**Fu** is close to the sum of the component absorption profiles, which would indicate a weak electronic coupling between the components; Fu-centered bands are present in the same regions, with an additional absorption tail extending at $\lambda > 600$ nm, a typical feature of this chromophore.[26,41] **Pt** and **PtCl** exhibit typical $\pi\pi^*$ and Pt → terpy ^{1}MLCT transitions in the ranges 300−360 nm and 360−450 nm, respectively;[9−14] **Pt**, in addition, presents peculiar bands in the region 450−550 nm that can be attributed to mixed Pt → terpy MLCT/π(C≡C) → π^*(tpy) LLCT transitions.[12,42]

Emission data for the **Pt**−**Fu** dyad and the component units at both room temperature and 77 K are collected in Table 2; results for the related complex **PtCl** are also listed. Regarding the latter, it is known that the spectroscopy, and particularly the luminescence, of [Pt(terpy)-Y]$^+$ systems is greatly affected by both the nature of the Y halide or pseudohalide and that of the groups appended to the terpy frame.[2] In our case, **PtCl** exhibits a weak emission ($\phi_{em} = 1.0 \times 10^{-4}$) that undergoes a blue shift, from 491 to 464 nm, upon going from room temperature to 77 K, in CH_2Cl_2 and MeOH/EtOH solvents, respectively, which is a behavior consistent with a MLCT nature of the emission. However, the resolved emission profile, particularly at 77 K, Figure 4, is also consistent with contributions from levels of a LC nature.[2] The presence of

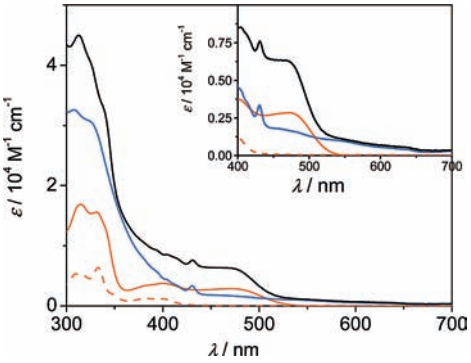

Figure 3. Absorption spectra of CH_2Cl_2 solutions of **Pt**−**Fu** (black), **Pt** (orange full), **Fu** (blue), and **PtCl** (orange dash).

a strong-field acetylide ligand in the fourth coordination position of platinum, as in **Pt**, raises the energy of the d−d states, enhancing luminescence over nonradiative decay; the emission of **Pt**, in fact, has a quantum yield of 0.013 in degassed CH_2Cl_2 solutions (Table 2). The emission maximum shifts from 605 to 523 nm in passing from room temperature to 77 K (Table 2 and Figure 5), and this luminescence is assigned to predominantly ^{3}MLCT character.[12] With regard to **Pt**−**Fu**, **Pt**, and **Fu**, Figure 5 compares emission spectra as observed at room temperature in CH_2Cl_2 and at 77 K in the MeOH/EtOH mixture. For **Pt**−**Fu**, and according to the absorption spectra displayed in Figure 3, use of $\lambda_{exc} = 450$ nm results in a 1.2:1 proportion of ^{1}Pt-centered (with subsequent very fast formation of ^{3}Pt states, $k_{isc} \geq 10^{12}$ s^{-1})[1] and ^{1}Fu-centered excited states. However, in air-free solvent, only the Fu-centered fluorescence is detected at room temperature, $\lambda_{max} = 708$ nm and $\tau = 1.2$ ns,[43] while no ^{3}Pt-centered emission is present, Table 2 and Figure 5. On the other hand, 450 nm excitation of isoabsorbing solutions of **Fu** and **Pt**−**Fu** in air-equilibrated solvent results in very similar $^1O_2$* fluorescence intensities, observed at 1278 nm, Figure 6. All of this is consistent with complete Pt → Fu energy transfer in the dyad, leading to final population of the ^{3}Fu level and subsequent $^1O_2$* sensitization for the air-equilibrated case.[26,27,43,44]

The excited state dynamics generated upon photoexcitation of the **Pt** moiety of **Pt**−**Fu** can be discussed with reference to the energy layout displayed in Scheme 1. Here, the ^{3}Pt, ^{1}Fu, and ^{3}Fu energy levels are estimated from the concerned emission peaks at 77 K, and that for the CS Pt$^+$−Fu$^-$ level, E_{CS}, is evaluated by using eq 2,[45]

$$E_{CS} = E'_{ox} - E'_{red} - \frac{e_0^2}{\varepsilon d} \qquad (2)$$

where ($E'_{ox} - E'_{red}$), e_0, ε, and d are the "redox energy" (eV), the electron charge, the solvent dielectric constant, and the intercenter distance, respectively. The last term of eq 2, an electrostatic factor, is evaluated to be 0.16 eV (d = 10 Å) in CH_2Cl_2 at room temperature, and E_{CS} = 2.03 eV

(39) Crites, D. K.; Cunningham, C. T.; McMillin, D. R. *Inorg. Chim. Acta* **1998**, *273*, 346–353.
(40) Hill, M. G.; Bailey, J. A.; Miskowski, V. M.; Gray, H. B. *Inorg. Chem.* **1996**, *35*, 4585–4590.
(41) Guldi, D. M.; Prato, M. *Acc. Chem. Res.* **2000**, *33*, 695−703.
(42) Yam, V. W. W.; Wong, K. M. C.; Zhu, N. Y. *Angew. Chem., Int. Ed.* **2003**, *42*, 1400–1403.
(43) Clifford, J. N.; Accorsi, G.; Cardinali, F.; Nierengarten, J. F.; Armaroli, N. *C. R. Chim.* **2006**, *9*, 1005–1013.
(44) Rio, Y.; Accorsi, G.; Nierengarten, H.; Bourgogne, C.; Strub, J. M.; Van Dorsselaer, A.; Armaroli, N.; Nierengarten, J. F. *Tetrahedron* **2003**, *59*, 3833–3844.
(45) Gaines, G. L.; Oneil, M. P.; Svec, W. A.; Niemczyk, M. P.; Wasielewski, M. R. *J. Am. Chem. Soc.* **1991**, *113*, 719–721.

Table 2. Photophysical Properties[a]

	295 K			77 K		
	λ_{max}[b] (nm)	ϕ_{em}[c]	τ[d] (ns)	λ_{max}[b] (nm)	τ[e] {ϕ_{em}}[f] (ns)	E[g] (eV)
PtCl	491	1.0×10^{-4} [1.0×10^{-4}]	1.3 [1.3]	464	9.8×10^3 {0.75}	2.67
Pt	605	0.013 [0.0047]	920 [313], τ_{TA} = 810[h]	523	20×10^3 {0.28}	2.37
Fu	708 [708, 1278[i]]	6.0×10^{-4} [5.3×10^{-4}]	1.2 [1.2], τ_{TA} = 24.8×10^3 [j]	703,[k] 820 [l]	1.1, –[m]	1.76
Pt–Fu	708 [708, 1278[i]]	6.6×10^{-4} [5.5×10^{-4}]	1.2 [1.2], τ_{TA} = 14.3×10^3 [j]	705,[k] 820 [l]	1.3, –[m]	1.76, 1.51

[a] Luminescence detected in CH_2Cl_2 solutions at room temperature (air-free solutions, in square brackets are values for air-equilibrated solutions) and in 1:4 MeOH/EtOH solutions at 77 K; transient absorption (TA) results obtained in CH_2Cl_2 solutions at room temperature, see Experimental Section. [b] Emission maxima, excitation at 330 and 450 nm. [c] Quantum yields, air-free solutions, determined by comparing emission spectra and using quinine sulfate in 1 N H_2SO_4 or $[Ru(bpy)_3]Cl_2$ in aerated water as standards; excitation at 330 or 450 nm (in square brackets are values for air-equilibrated solutions). [d] Lifetimes; air-free solutions; excitation at 331, 465, or 560 nm for the emission (in square brackets are values for air-equilibrated solutions); for the decay of the TA, λ_{exc} was 450 nm. [e] Emission lifetimes, excitation at 331, 465, or 560 nm. [f] In brackets are quantum yields (estimated with a large uncertainty, 30%). [g] Energy level of the emitting state, from the highest energy emission peak of the spectrum at 77 K. [h] From TA spectroscopy, decay observed at 790 nm, see Figure 7. [i] For sensitized $^1O_2$* emission, see text. [j] From TA spectroscopy, decay observed at 680–690 nm, see Figure 6. [k] Fluorescence from the ^{1}Fu state. [l] Phosphorescence from the ^{3}Fu state. [m] No phosphorescence lifetime detected.

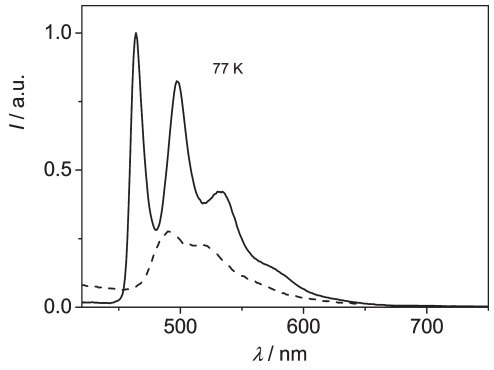

Figure 4. Arbitrarily normalized emission spectra of **PtCl** at room temperature in CH_2Cl_2 (dash) and at 77 K in MeOH/EtOH (1:4 v/v) glass (full); excitation at 330 nm.

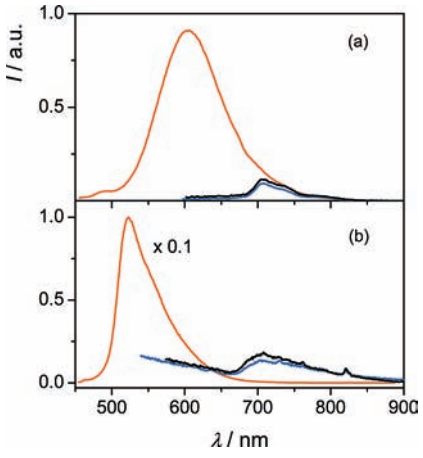

Figure 5. Emission spectra of isoabsorbing solutions at λ_{exc} = 450 nm of dyad **Pt–Fu** (black) and components **Pt** (orange) and **Fu** (blue), at room temperature in CH_2Cl_2 solvent (a) and at 77 K in MeOH/EtOH (1:4 v/v) glassy solutions (b).

(for **Pt–Fu**, E_{ox} = +1.42 V and E_{red} = −0.77 V, vs SCE, Table 1).

The fact that excitation of isoabsorbing solutions of **Fu** and the dyad **Pt–Fu** at the same wavelength yields comparable Fu- or $^1O_2$*-centered luminescence intensity (Figures 5 and 6, Table 2) might be consistent with both (i) complete Pt → Fu energy transfer within the latter and

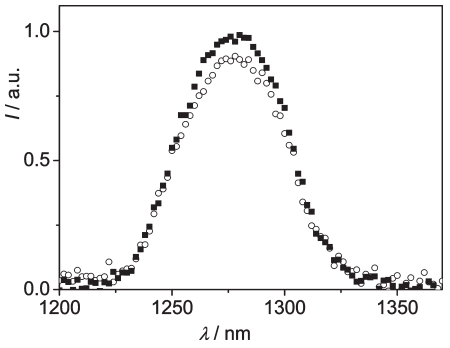

Figure 6. Emission spectra observed with λ_{exc} = 450 nm for air-equilibrated isoabsorbing CH_2Cl_2 solutions of **Pt–Fu** (■) and Fu (○); absorbance = 0.36.

Scheme 1. Energy of the Excited Levels (in eV) in Dyad **Pt–Fu**[a]

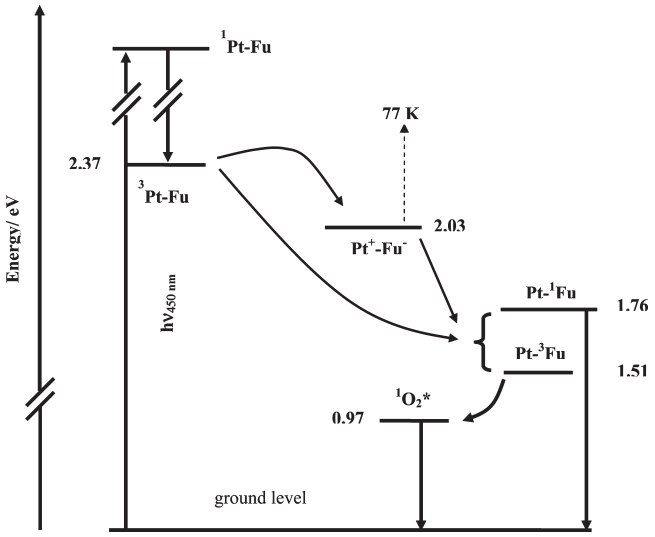

[a] CS or CT levels entirely located at the Fu unit could lie close to Pt^+-Fu^-, see note of ref 46. Luminescence and TA spectroscopy only reveal fluorescent (Pt–^{1}Fu) and phosphorescent (Pt–^{3}Fu) dyad-based levels or $^1O_2$* levels (for air-equilibrated solutions).

(ii) electron transfer, ^{3}Pt–Fu → Pt^+–Fu^-,[46] followed by fast deactivation to yield ^{1}Fu fluorescence and ^{3}Fu phosphorescence, the ^{1}Fu → ^{3}Fu step taking place practically

with unit efficiency.[44,47,48] The observation that fullerene-based fluorescence (λ_{max} = 705 nm, τ = 1.3 ns),[43] and phosphorescence (a sharp peak, λ_{max} = 820 nm, no lifetime detected),[28] is registered at 77 K (Figure 5b) is interesting. In a glassy solution at 77 K, even if the internal reorganization energy at the Fu fragment is small,[41] the barrier to electron transfer is expected to increase by an amount on the order of 0.5 eV,[45,49,50] because of outer-sphere contributions of a solvent origin. This would place the Pt^+-Fu^- CS state at >2.5 eV so that the energy content of the ^{3}Pt level, 2.37 eV, would not be enough to drive electron transfer. In conclusion, upon 450 nm excitation of the Pt moiety of **Pt**−**Fu** and formation of ^{3}Pt-centered excited states, the luminescence results are well accounted for by an overall complete Pt → Fu energy transfer, and no evidence for CS state formation is found. This is further corroborated by transient absorption (TA) results, as discussed below.

Figure 7 shows room-temperature TA spectra registered at the end of the pulse for the dyad **Pt**−**Fu** and reference **Pt** and **Fu** components, upon excitation of air-free CH_2Cl_2 isoabsorbing solutions at 450 nm. In the inset, the time evolution of the transient absorbance of dyad **Pt**−**Fu** and those of the relative models are shown. The TA spectrum of **Pt**, attributed to the ^{3}Pt state, is well-separated from those of **Pt**−**Fu** and **Fu**. It peaks around 770 nm and decays with τ_{TA} = 810 ns. The spectral profile closely resembles that recently reported by Castellano et al. for a similar Pt−acetylide complex,[10] and the lifetime is in good agreement with the ^{3}Pt luminescence result, Table 2. With regard to **Pt**−**Fu** and **Fu**, their TA spectra exhibit very similar profiles with peaks at 680 and 690 nm and τ_{TA} = 14.3 and 24.8 μs, respectively; on these bases, the spectra are attributed to absorption by localized $^3C_{60}$ states both in **Pt**−**Fu** and in **Fu**.[27,51] The different τ_{TA} values in the two cases point to somewhat different electronic conditions for the Fu unit in **Pt**−**Fu**, as already observed for dyads containing heavy-metal Ru- and Re-based components.[27] The results illustrated in Figure 7 indicate that ^{3}Fu is the final excited state produced in **Pt**−**Fu**. In particular, the typical peak of the reduced fulleropyrrolidine species, Fu^-, falling in the range 1010−1050 nm and showing a strong dependence on the solvent,[24,41,52,53] is not detected. Of course, this is not definite evidence for the lack of formation of the CS separated Pt^+-Fu^- species in **Pt**−**Fu**, because its lifetime could be too short to be observed on the time scale

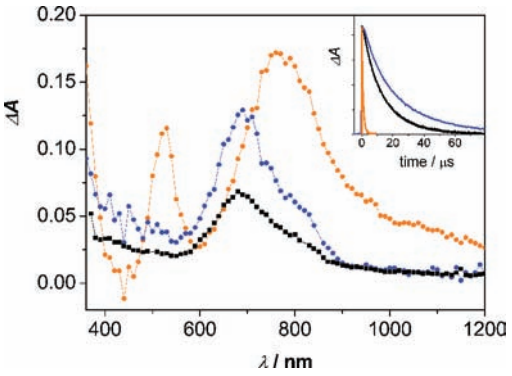

Figure 7. Room temperature end-of-pulse TA spectra registered upon excitation at 450 nm of isoabsorbing (A_{450} = 0.45), degassed CH_2Cl_2 solutions of **Pt**−**Fu** (black), **Fu** (blue), and **Pt** (orange). In the inset, the time evolution of the transient absorbance of **Pt**−**Fu** at 680 nm (black), **Fu** at 690 nm (blue), and **Pt** at 790 nm (orange) are shown.

employed here.[52] As seen above, the Pt^+-Fu^- lowest-lying level is evaluated to lie at 2.03 eV and, therefore, is lower in energy than ^{3}Pt−Fu, 2.37 eV.[11] Thus, the CS Pt^+-Fu^- species could in principle be produced upon excitation of the Pt(terpy) unit, with a $\Delta G°$ of ca. −0.34 eV. The lack of observation of this level could be explained either by admitting that it is too short-lived (that is, by an inadequacy of our instrumentation) or because of reasons given below.

First of all, we note that deactivation of the Pt^+-Fu^- level to reach the ground level via charge recombination (CR) should be a slow process, given that the high energy of the CS level places the process inside the Marcus inverted region.[54] By contrast, fast CR steps might occur by population of the lower-lying excited states (singlet or triplet, $\Delta G°$ = −0.27 and −0.52 eV, respectively) of the fullerene moiety, see Scheme 1. The ^{1}Fu and ^{3}Fu luminescent levels of **Pt**−**Fu** are in fact detected at room temperature by luminescence and TA spectroscopy (see above). As mentioned above, at 77 K, the Pt^+-Fu^- CS state is expected to be destabilized by an amount of ca. 0.5 eV,[45,49,50] which should definitely prevent its population in **Pt**−**Fu**.

Second, the energy transfer steps ^{3}Pt → ^{1}Fu and ^{3}Pt → ^{3}Fu are energetically allowed, since they are exothermic by ca. 0.61 and 0.86 eV, respectively (Scheme 1). The former is formally forbidden in terms of spin-multiplicity, but it is well-known that the heavy Pt center renders the process allowed via spin−orbit coupling.[1] The latter instead is spin-allowed. A detailed analysis of the ^{3}Pt → ^{1}Fu energy transfer process in terms of Dexter[55] and Förster[56] mechanisms is allowed by the available spectroscopic data, and one sees that both mechanisms provide an energy transfer rate constant $k_{en} > 10^7$ s^{-1} (see the Supporting Information). According to the former mechanism, the spectral overlap between the luminescence profile $F(\bar{\nu})$ of Pt and the absorption profile $\varepsilon(\bar{\nu})$ of Fu is evaluated $J^D = 7.5 \times 10^{-5}$ cm. In dyad **Pt**−**Fu**, the Pt and Fu centers are ca. 10 Å far apart and separated by a rigid interposed linker (Chart 1). Even if this linker does not allow a strong interaction between the component units, for a really small interaction term, say $H \sim 0.5$ cm^{-1}, k_{en}^D

(46) As suggested by the electrochemical results, a CS or CT level, possibly of a pyrrolydine-to-fullerene nature, could formally be located at the Fu unit. However, we disregard any discussion of a possible role for this level because its deactivation to ^{1}Fu- or ^{3}Fu would presumably be a very fast process given its localized nature.

(47) Redmond, R. W.; Gamlin, J. N. *Photochem. Photobiol.* **1999**, *70*, 391–475.
(48) Wilkinson, F.; Helman, W. P.; Ross, A. B. *J. Phys. Chem. Ref. Data* **1993**, *22*, 113–262.
(49) Closs, G. L.; Johnson, M. D.; Miller, J. R.; Piotrowiak, P. *J. Am. Chem. Soc.* **1989**, *111*, 3751–3753.
(50) Chen, P. Y.; Danielson, E.; Meyer, T. J. *J. Phys. Chem.* **1988**, *92*, 3708–3711.
(51) Allen, B. D.; Benniston, A. C.; Harriman, A.; Mallon, L. J.; Pariani, C. *Phys. Chem. Chem. Phys.* **2006**, *8*, 4112−4118.
(52) Guldi, D. M.; Maggini, M.; Scorrano, G.; Prato, M. *J. Am. Chem. Soc.* **1997**, *119*, 974–980.
(53) Fujitsuka, M.; Ito, O.; Yamashiro, T.; Aso, Y.; Otsubo, T. *J. Phys. Chem. A* **2000**, *104*, 4876–4881.
(54) Marcus, R. A.; Sutin, N. *Biochim. Biophys. Acta* **1985**, *811*, 265−322.
(55) Dexter, D. L. *J. Chem. Phys.* **1953**, *21*, 836.
(56) Förster, T. *Discuss. Faraday Soc.* **1959**, *27*, 7.

is evaluated $\sim 10^8$ s^{-1}.[57] With regard to the Förster mechanism,[56] the spectral overlap between the luminescence profile $F(\bar{\nu})$ of **Pt** and the absorption profile $\varepsilon(\bar{\nu})$ of **Fu** affords an overlap integral $J^F = 6.9 \times 10^{-15}$ cm^3 M^{-1}, a critical transfer radius $R_o = 15.3$ Å, and $k_{en}{}^F = 1.4 \times 10^7$ s^{-1} at an intercomponent separation $d = 10$ Å (results for room temperature and further details are available in the Supporting Information).

Given that, in the reference **Pt** complex, the phosphorescence is rather long-lived, $\tau \sim 0.9$ and 20 μs at room temperature and at 77 K, respectively (Table 2), energy transfer can account for the observation of the full quenching of the Pt-based luminescence in the **Pt**−**Fu** dyad, eq 3.

$$\frac{I_0}{I} = 1 + k_{en}\tau_0 \qquad (3)$$

Here, I_0 and I are the Pt-based luminescence intensities of **Pt** and **Pt**−**Fu**, respectively, and τ_0 is the luminescence lifetime of **Pt**. The drawn $I_0/I \geq 13.6$ (at room temperature) corresponds to the observed quenching of the Pt-based luminescence in the dyad.

Conclusions

Here, we report on the synthesis, characterization, and study of the electrochemical and photophysical properties of a fulleropyrrolidine−acetylide−platinum(II)−terpyridyl dyad, the first case wherein a Pt(II)−terpyridine unit is linked to fullerene. The preparation of the target dyad requires cross-coupling between a Pt precursor and a Fu derivative adequately functionalized respectively with a chloride and a terminal alkyne. Upon excitation of the Pt(terpy) center of **Pt**−**Fu**, a complete Pt → Fu energy transfer process is operative both at room temperature and at 77 K. The energy transfer processes ^{3}Pt → ^{1}Fu and ^{3}Pt → ^{3}Fu are, in fact, both energetically allowed, and the former can be discussed in terms of Dexter[55] and Förster[56] mechanisms by using the available spectroscopic results. In principle, the CS Pt^+-Fu^- species could be produced upon excitation of the Pt(terpy) unit, but we failed its detection. This can be explained by the inadequacy of our instrumentation (in the case of a very short lifetime) or by the occurrence within the **Pt**−**Fu** dyad of fast CR steps that populate the lower-lying luminescent levels of ^{1}Fu and ^{3}Fu nature, as actually observed.

Acknowledgment. Funding from CNR of Italy (PM. P04.010, Project MACOL), MIUR (FIRB RBIP0642YL, Project LUCI; FIRB RBIP0642YL, Project NODIS), CNRS, and ANR FCP-OLEDs No.-05-BLAN-0004-01 are acknowledged.

Supporting Information Available: Analysis of the energy transfer processes that occur in dyad **Pt**−**Fu** in terms of Dexter and Förster mechanisms. This material is available free of charge via the Internet at http://pubs.acs.org.

(57) Barigelletti, F.; Flamigni, L. *Chem. Soc. Rev.* **2000**, *29*, 1–12.